

# CFD Simulation of Different Taper Ratio Wings, Performing Trade-off Assessment and Development of A New Methodology to Plot Lift Distribution Curve and 3D Local Coefficient of Lift Distribution Graph

Mr. Tejas Dhekane <sup>a</sup>, Dr. Nitin Sherje <sup>b</sup>

<sup>a,b</sup> Department of Mechanical Engineering,  
SKNCOE, Savitribai Phule University,  
Pune

**Abstract:** Tapered wing plan form dominates the wing design mainly because of its manufacturability, low induced drag, fewer tip vortices and an increase in the lift which accounts in the increase in the overall efficiency of the Wing. In this paper Selig's S1223 aerofoil was used and wings with various different Taper ratios have been designed and developed in CATIA V5 and were analysed in the ANSYS FLUENT 16.0 and MATLAB software. The new methodology to plot the lift distribution curve and the Local coefficient of Lift distribution curve was developed and tested and a database of Lift Distribution graph and local coefficient of lift distribution graph was generated. A detailed trade study was performed on the basis of lift distribution, the local coefficient of lift distribution and structural strength..

**Keywords:** Wing Design, Tapered-Wings, Taper Ratio, Lift Distribution, Coefficient of Lift, Computational Fluid Dynamics.

## 1) INTRODUCTION

### 1.1 Motivation

RC planes have started to captivate the global markets in recent years. Development of light weight batteries, Powerful small sized cameras and the development of stabilization systems are the main reason for this development. RC planes have wide applications and many are still under research. Defence sector is at the forefront in the research as these tiny machines can turn into a deadly weapon within some fractions of a second. Delivery services are currently developing a business models using these machines. There are many people who fly the planes as a part of their hobby. The applications are boundless so in order to explore this upcoming field of RC planes, there was a need of some platform where we could gain and experiment on some things, try and develop our own wing designs. We participated in one such competition and the whole process motivated me to explore this sector more.

### 1.2 Basics

Wings are the basic and most important part of any commercial as well as RC plane. Wings have a particular shape which produces the lift that can sustain the weight of an aeroplane in the air. The pilot controls the movement of aircraft using the special control surfaces that are located on the wings. Wings produce lift using the combination of Coanda Effect and the Newton's Third Law of Motion. [1] Coanda effect explains us the behaviour of fluid particles around any object or curved body. Air being a fluid follows the Coanda Effect and sticks up to the aerofoil till the end. Aerofoils have a characteristic design and they tend to taper at the trailing edge causing the air stream to bend down as it flows. When the air bends around the surface of the wing it tries to separate from the airflow above it. But since air has strong reluctance to form voids, attempt to separate lowers the pressure and bends the adjacent streamlines above. This Lowering of the pressure propagates out at a speed of sound, causing a great deal of air to bend around the wing. This produces a low-pressure region on the upper surface of the wing and downwash is produced. Lift depends on the shape of an aerofoil and so does the Drag Force and hence the selection of aerofoil and wing design are the most crucial part of the design of a RC plane.

### 1.3) Aerofoil Terminology

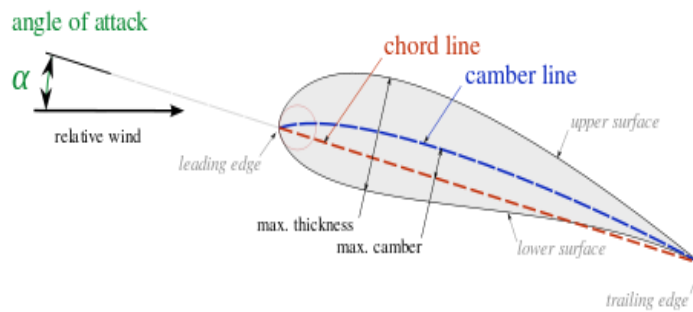


Figure 1 : Aerofoil Terminology

The basic aerofoil shape is shown in fig 1 [2] which illustrates the basic terminology of the aerofoils.

- **Leading edge:** It is the frontmost edge of an aerofoil.
- **Trailing edge:** It is the rearmost edge of an aerofoil.
- **Camber line:** A curve drawn in between the upper and lower surfaces of the aerofoil such that it is equidistant from both the surfaces at any point.
- **Chord line:** A straight Line Connecting the Leading and Trailing edge of the aerofoil.
- **Thickness:** It is the maximum perpendicular distance between the Upper and Lower surface of an aerofoil.
- **Angle of attack (AOA):** It is defined as the angle between the chord line and the relative wind or flight path.

### 1.4) Downwash and its effects

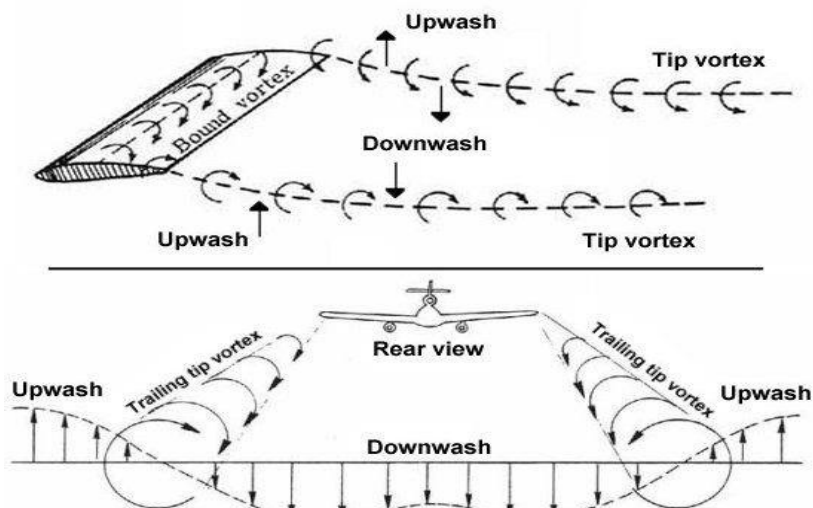


Figure 2: Downwash

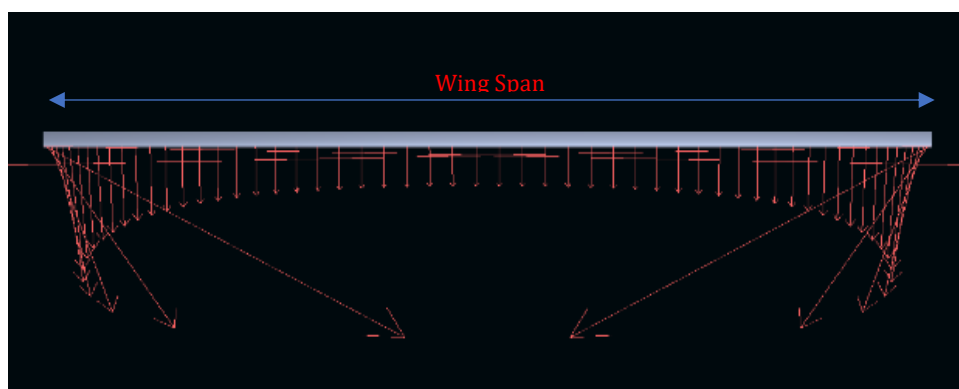


Figure 3 : Downwash Distribution across the span.

As the pressure difference exists between the upper and Lower sides of an aerofoil, the high-pressure air tries to curl up around the wing tips forming the trailing edge vortex sheets which results in the trailing tip vortices as explained in Figure 2. [3] Lifting Line theory expresses Wing as the Vortex Sheet and lift can be calculated by the Kutta-Joukowski theorem. A profile of downward force along the span which is the result of trailing edge vortices and the vortex sheet is known as downwash. Fig 3 depicts the profile of Downwash over the span of a finite 3D rectangular wing. Maximum Downwash can be seen at the tips and minimum at the centre for a rectangular Wing. This downwash distribution has many consequences and is the prime factor in deciding the efficiency of a particular wing. The wingspan is denoted by 'y' and we can say that the downwash is the function of wingspan.

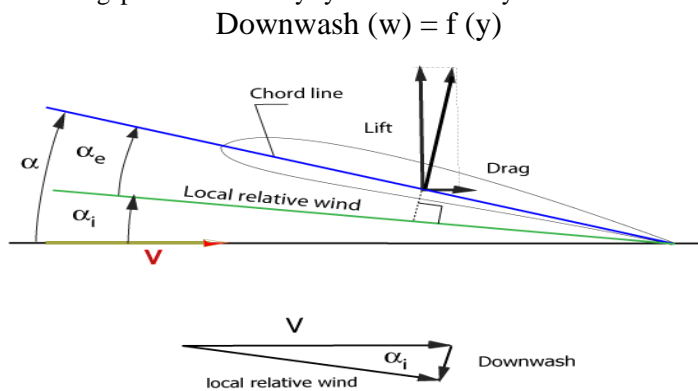


Figure 4 : Effective and Induced Angle of Attack.

Referring the fig 4. [4]

- Vector  $V$  = direction and magnitude of free air stream Velocity.
- $\alpha$  = Geometric Angle of Attack.
- $\alpha_i$  = Induced Angle of Attack
- $\alpha_e$  = Effective Angle of Attack.

$$\alpha_e = \alpha - \alpha_i$$

Thus, as we move towards the tip of the wings for a rectangular wing, downwash increases and so does the induced angle of attack. Hence the effective Angle of Attack decreases which decreases the lift in the vertical direction and increases the drag along the direction of the air velocity. This drag is known as Induced Drag. We cannot avoid it as it is a by-product of the lift. Induced Drag decreases the efficiency of the wing as it requires more thrust power to overcome it and hence consumes more fuel. The maximum portion of the total drag generated by the wing comprises of the induced drag and hence it is very important to find ways in order to avoid it or find better solutions to avoid it or reduce it.

As the effective angle of attack decreases as we move towards the tip, the lift generation per unit area also decreases. This reduces the local coefficient of Lift  $cl(y)$  and a profile of  $cl(y)$  can be plotted.

$$cl(y) = \frac{Lift \times 2}{\delta \times A \times V \times V}$$

- Local lift coefficient ( $cl(y)$ ) = Coefficient of Lift per unit area at a distance  $y$  from the centre of the wing.
- $\delta$  = Density of Fluid, air in this case. ( $kg/m^3$ )
- $A$  = Wing Area ( $m^2$ )
- $V$  = Relative Velocity (m/s)

Thus, the Lift Distribution is the main aspect and very important part of wing designing.

### 1.5) Remedies to the Induced Drag Problems

The Elliptical Lift Distribution is the best-known solution to the induced drag problem as it offers the least induced drag. Many of the aircraft during world war 2 had elliptical wings like Submarine Spitfire. These wings were very difficult to manufacture and this was the major reason for their downfall. Further People understood that elliptical lift distribution can be obtained using the Taper Wings with certain modifications to it. Basic Idea that revolves around the Taper wings is if the Downwash is maximum at the tips for rectangular planform then if we provide lesser tip chord and increase the root chord proportionally then we can have the lower the induced drag but the same wing area thus increasing the efficiency of the wing. Thus, the Idea of Taper Wing

evolved. Taper ratio is the ratio of the root chord and the tip chord but the problem arises when we have to perform the trade studies while selecting a particular taper ratio for a particular application. The paper revolves around a similar subject.

### 1.6) Taper Wing Terminology and Basics

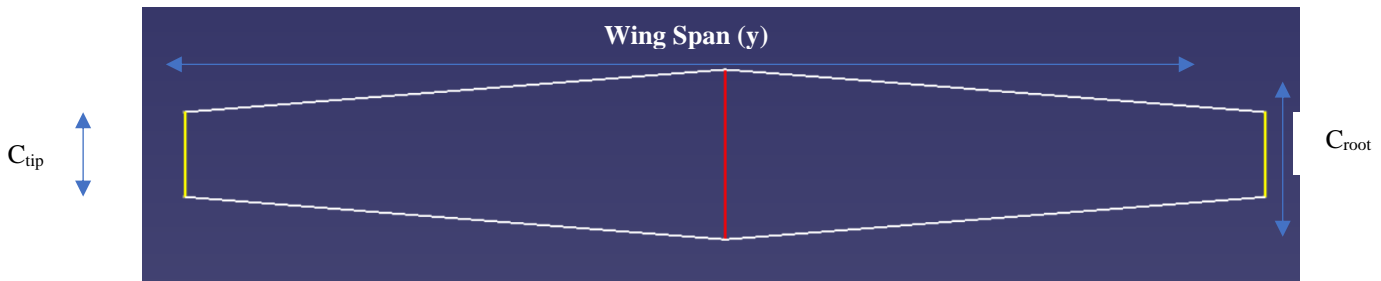


Figure 5 : Common tapered wing

- Wing Span = (y)
- Root Chord =  $C_{root}$
- Tip Chord =  $C_{tip}$
- Mean Aerodynamic Chord = MAC
- Aspect Ratio =  $\frac{y}{MAC}$
- Taper Ratio (  $\lambda$  ) =  $\frac{C_{root}}{C_{tip}}$

Many of the Aerodynamic properties depend on the above characteristics of the wing. Lift is proportional to the Wing Area, stalling characteristics depend on the Aspect Ratios, Induced Drag depends on the Aspect Ratio too. Thus to compare any two wings, we need to make certain arrangements and make sure that the comparison parameters are same and they start from a common ground.

### 2) PAPER OBJECTIVE

There are many parameters that we must take into consideration while designing a plane. While designing a tapered wing there are many things which vary if we just change the taper ratio. These changes have an effect on the performance of the wing. In this paper, we aim to perform the trade studies for the wing with different taper ratios but same wing area, A]aspect ratio, twist angle, washout angle, polyhedral angle and angle of attack so that we have a common base to compare the different wings. We intend to analyse each wing on the CFD Fluent Solver and plot the local lift coefficient  $cl(y)$  graph using the Matlab Software and find the best suitable taper ratio which is suitable for our application. Lastly, we aim to establish a new methodology which can be used to plot local lift coefficient  $cl(y)$  graphs for different wings using the CFD Fluent and the Matlab Software and generate a database of the results of wings with different Taper Ratios.

### 3) OVERALL APPROACH

A Lift can be defined as the force which opposes the weight force. Lift produced by the aerofoil can be given by the formula,

$$Lift = \int_0^c (Pl(x) - Pu(x)).dx$$

In the above equation, 'c' denotes the chord length and 'dx' denotes the thickness of an aerofoil.  $Pl(x)$  denotes the pressure on the lower surface of an aerofoil  $x$  distance away from the reference point while  $pu(x)$  denotes the pressure on the upper surface of an aerofoil  $x$  distance away from the reference point. Now if we could manage to plot the pressure distribution curve properly then we can find the lift very easily. As the pressure distribution is not constant over the entire span, we use the basics of integration. Firstly, we have to find a way to divide the half span into number of blocks and then use the above formula to formulate the lift generated by the each individual block giving us an idea about the lift distribution by individual blocks and then add it up to find the total lift and also the Overall Lift distribution.

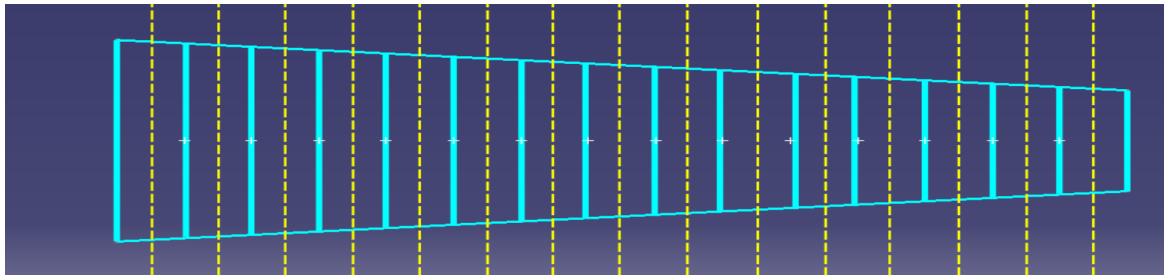


Figure 6 : Half wing divided into small blocks.

Like in figure 6 we can divide our half wingspan into a number of parts which is shown in blue colour and a yellow line is drawn at the centre of each block where pressure plot will be generated assuming that the entire block shares the same pressure distribution across the chord. It's an assumption that we are considering but as the number of divisions goes on increasing the accuracy of prediction increases and vice versa.

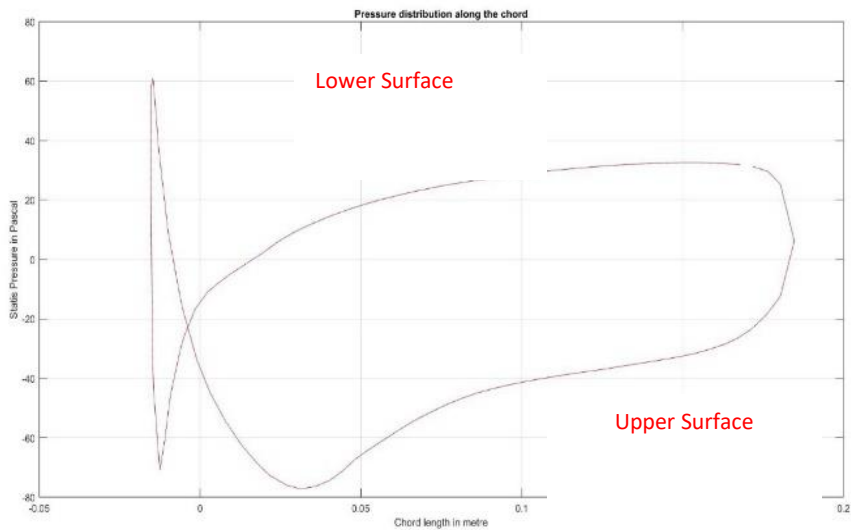


Figure 7 : Pressure Distribution Curve for a S1223 aerofoil.

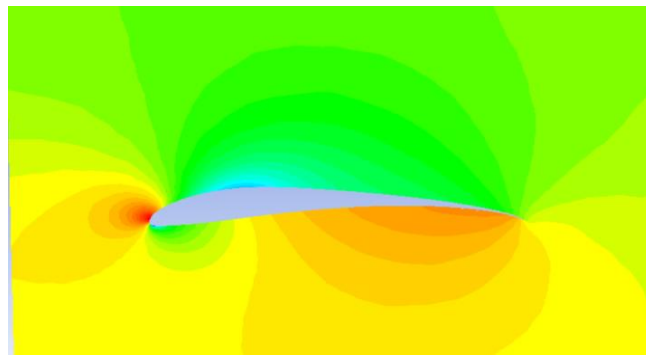


Figure 8 : Pressure Contours for S1223 aerofoil.

Figure 7 represents the pressure distribution curve of Selig S1223 aerofoil at 0° Geometric Angle of Attack. We know that the upper surface of an aerofoil has low pressure and the lower surface of an aerofoil has high pressure. We can clearly see that in the pressure contour plot in figure 8.

Now the Pressure contours were exported and accessed through Matlab Software where we integrated the integral and found out the area enclosed in between the curve. When we multiply it with the thickness of a block, we get a lift generated by each individual block. When we add the lift generated by individual block then we can find out the total lift generated. Next Step, we know that Lift can also be found out using a simple formula,

$$Lift = \frac{1}{2} \times \delta \times A \times V \times V \times Cl \quad cl(y) = \frac{Lift \times 2}{\delta \times A \times V \times V}$$

Now, after we found out the lift generated by each individual block, we can use the above formula and calculate the value of Coefficient of Lift Cl and then we can plot the lift distribution graph. This graph will help us study the basic characteristics of the RC plane. It will help us find the values of 3D Cl, its L/D ratio, Stalling Patterns, Induced Drag distribution. Hence, the basic aim of this paper is to perform the trade studies and decide the Value of Taper Ratio which is optimized in all senses.

#### 4) METHODOLOGY

##### 4.1) Prerequisites

To carry on with the research paper we decided a few things beforehand. We decided to perform the trade studies for the RC planes and so finalized the wing area of 2400cm<sup>2</sup>. This wing area was appropriate for the RC plane wing. We also decided to go with the most common aspect ratio of 6. This was done to reduce the errors. Now we plot a table 1 and find the dimensions of root chord and tip chord as well as the length of the tapered-wings while maintaining the same wing area and aspect ratio but



We have the values of characteristic lengths ranging from 32.87cm to 3.827 cm. Accordingly, we have a range of Reynolds number from 2,19,200 to 21,900. The coefficient of lift vs angle of attack graph is influenced by the Reynolds number and the values of all coefficient of lift values are in between these two limits of Reynolds number.

#### 4.2) CFD Analysis using Ansys Fluent.

The CFD analysis is mainly divided into 3 stages namely pre-processing, processing and post-processing stage. In the pre-processing stage, the 3D-model is developed in the Cad Software and exported to analysing software where meshing is performed and the boundary conditions are set according to the problem statement. In the processing part, the software solves the problem using the finite volume method with according to the constraints and gives out the solution to the problem statement. There are many such solvers available with the software, we have to analyse the problem and finalize the solver which best suits our application. Lastly, in the post-processing stages, we have to present the solution which everybody can understand easily usually in pictorial representations like graphs, contours curves, animations etc and also find out the values of the solution to the stated problem statement. In this case mainly the lift and drag forces and the respective coefficients.

#### 4.3) Pre-Processing

##### 4.3.1) Model Generation

Using the data which we finalized in the previous step, we designed the 3D models of all the wings using the CAD software CATIA V5. Figure 6 is a model of wing with the Taper Ratio of 0.5. The root chord of 26.17cm and the tip chord of 13.08 were imported from the database of S1223 air foil and then profiled with the Multi-section command followed by the mirror command and created as a single entity using the Boolean add command.

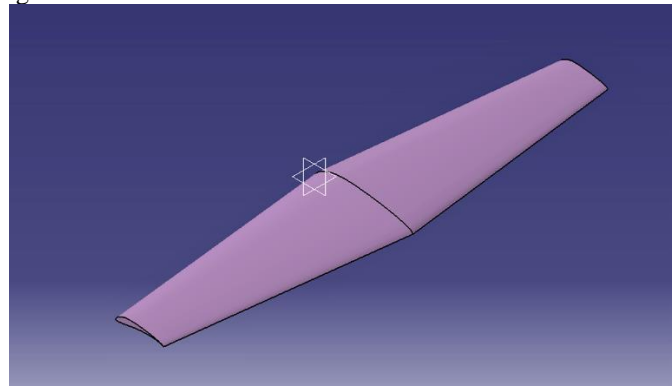


Figure 10 :Geometric Model of tapered wing generated in Catia V5

##### 4.3.2) Design of Fluid Domain

The model was then exported to Ansys Workbench 16.0 and the flow domain or the enclosure was designed in design modeler. The C section enclosure is commonly used and is known to replicate conditions which are closer to the real life. The Boolean operation was used to subtract the solid wing from the fluid domain which is a prime requirement of the finite volume method. The aerofoil faces were name selected so that we can plot the different pressure contours onto the aerofoil surface in the later parts of the analysis.

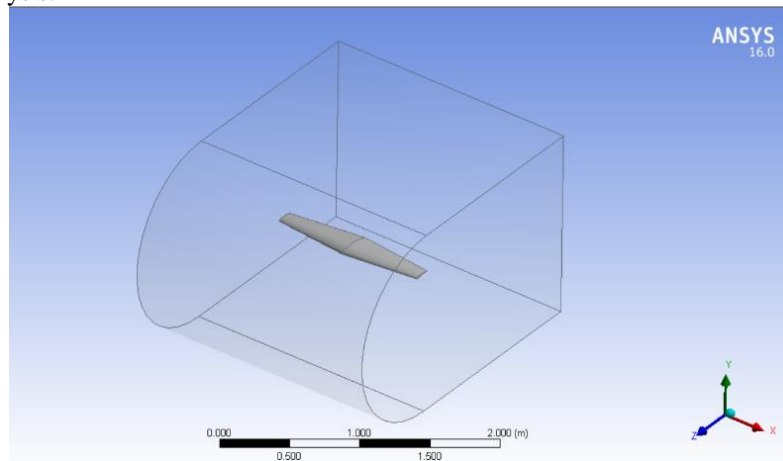


Figure 11 : C section enclosure around the aerofoil generated in Design Modeler in Ansys Workbench 16.0

##### 4.3.3) Grid Generation

The Grid Generation was performed in ICEM CFD Software in Ansys Workbench. We grid generated consisted of Tetrahedrons elements with a finer mesh and 20 layers of inflation added around the aerofoil with the growth rate of 1.2. The enclosure is face

meshed and the face sizing of the aerofoil was chosen to be 5mm while that of the enclosure was chosen to be 30mm. The main reason for using the tetrahedral mesh was that it takes less computational time while keeping in mind the accuracy and since the aerofoil is a complex shape the tetrahedral mesh is the best option.

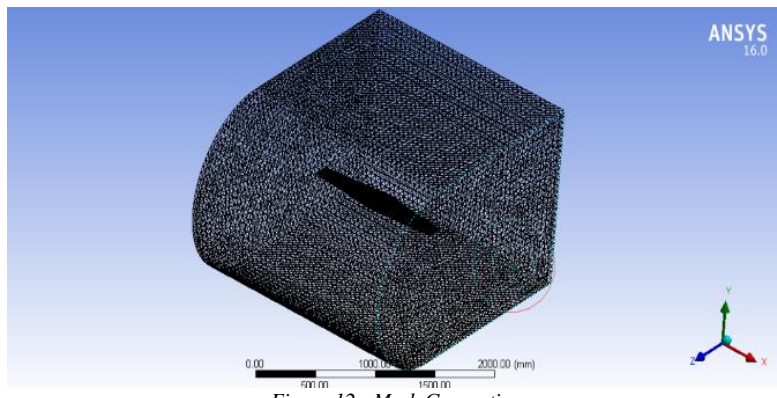


Figure 12 : Mesh Generation

#### 4.4.4) Boundary Conditions and Solver

The boundary conditions were set up in the Fluent Solver and the pressure-based solver was chosen as we were performing the analysis at a very low mach number approximately 0.029 mach where density will remain almost constant. The analysis was performed at the stalling speed of an RC plane because it gives us the fair idea about the lift and drag forces and also about the performance. Spalart-Allmaras was selected as the turbulence model because of low mach number and one-equation turbulence model that provide superior accuracy around boundary wall and unstructured mesh with much less computational time. [6] Plus, this model was specifically developed for the analysis of aerofoils and wings. Boundary conditions were set up as the inlet velocity with velocity assigned using the cartesian system and it was normal to the aerofoil in the negative Z direction with a magnitude of 10m/s and pressure outlet was set up as normal atmospheric conditions. Aerofoil and other faces of enclosures were also set up as walls. The second order upwind discretization was used for momentum and modified turbulent viscosity and reference values were calculated from the velocity inlet. The force monitors were applied in the respective directions to calculate the lift and drag and the solution was initiated with all the values taken with reference to the inlet velocity. The iteration process was started and the solution converged.

#### 4.4) Post Processing

After the solution converged, we divided the half wing into 15 blocks mathematically and highlighted an aerofoil at the centre of each part which will help us study that particular block better. In the Figure 14, half wing is divided into exact 15 blocks and the yellow highlighted line represents the position of highlighted air foil which will help us understand the properties of that respective block better. [7] To know the exact position of highlighted aerofoil we designed an algorithm in MS-Excel . Figure 15 will give us an idea about the algorithm which we had developed and its outcomes.

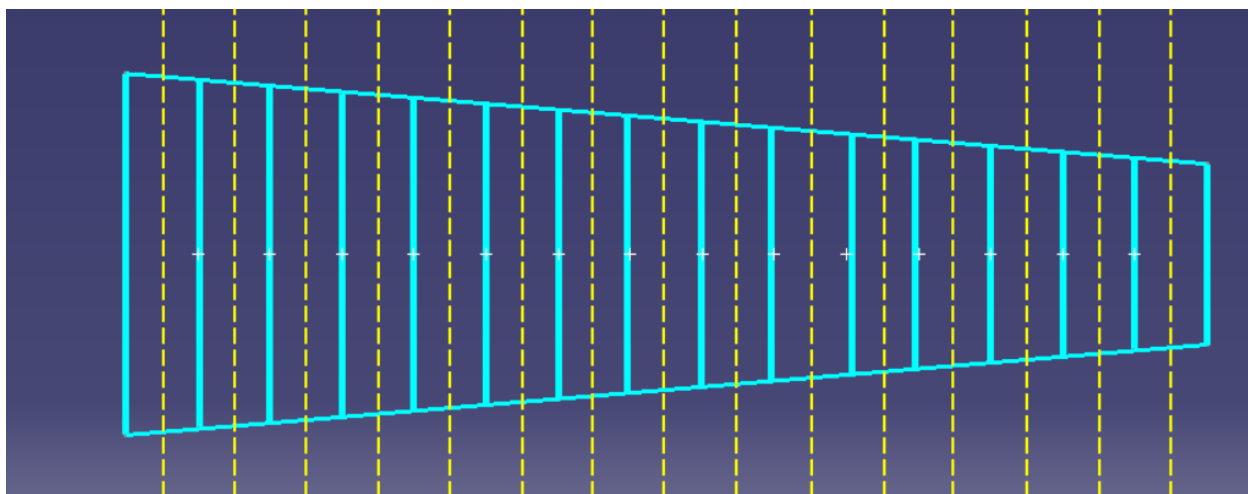


Figure 13 : : Half wing divided into small blocks.

		Wing Area Divisions							
1									
2	Taper ratio	0.5							
3									
4	Inputs	(cm)							
5			Theta =	0.1067 (Radians)		Tan function=	0.872653		
6	Root chord	26.1796	Theta =	6.1156 (degree)		Half Chord =	2.03721		
7	Tip Chord	13.0898	No. of points =	14					
8	Half Span	61.1163	Single Chord =	4.0744 (cm)		Single Chord	0.040744 (m)		
9	No. of divisions	15							
10									
11									
12	Area Number	Vertical Divisions	Area(cm <sup>2</sup> )	Area(m <sup>2</sup> )	Points(cm)	Points(m)	Parts(cm)	Parts(m)	Part No.
13	Root Chord	26.17960275	104.8889	0.010489	2.0372	0.020372	4.07442	0.040744	1
14	1	25.30694932	101.3334	0.010133	6.1116	0.061116	8.14884	0.081488	2
15	2	24.4342959	97.77781	0.009778	10.186	0.101861	12.22326	0.122233	3
16	3	23.56164247	94.22225	0.009422	14.26	0.142605	16.29768	0.162977	4
17	4	22.68898905	90.66669	0.009067	18.335	0.183349	20.3721	0.203721	5
18	5	21.81633562	87.11114	0.008711	22.409	0.224093	24.44652	0.244465	6
19	6	20.9436622	83.55558	0.008356	26.484	0.264837	28.52094	0.285209	7
20	7	20.07102877	80.00002	0.008	30.558	0.305582	32.59536	0.325954	8
21	8	19.19837535	76.44447	0.007644	34.633	0.346326	36.66978	0.366698	9
22	9	18.32572192	72.88891	0.007289	38.707	0.38707	40.7442	0.407442	10
23	10	17.4530685	70.33335	0.006933	42.781	0.427814	44.81862	0.448186	11
24	11	16.58041507	65.7778	0.006578	46.856	0.468558	48.89304	0.48893	12
25	12	15.70776165	62.22224	0.006222	50.93	0.509303	52.96746	0.529675	13
26	13	14.83510822	58.66668	0.005867	55.005	0.550047	57.04188	0.570419	14
27	14	13.9624548	55.11113	0.005511	59.079	0.590791	61.1163	0.611163	15
28	Tip Chord								
29									

Figure 14 : Self-Generated Algorithm for dividing Wings into equal Parts.

The inputs to the algorithm are root chord, tip chord and half span. Using the basic trigonometry and geometry we divided the half-wing into small blocks. The Blue Highlighted points in figure 15 are the coordinates where iso-surface along the z-axis on the aerofoil are marked. A yellow highlighted aerofoil represents the entire block and all the properties of that particular block will be represented by this particular aerofoil. Now after we have highlighted each aerofoil, we plot a graph of static pressures vs the chord in Ansys Fluent. We export the plots and open and save them in MS-excel sheets to access them using the Matlab Software. The figure 16 shows the Aerofoils highlighted along with the pressure contours. The figure 17 shows the static pressure vs chord length plot of 1st and 15th Aerofoil. The 18 last figure shows the static pressure graphs for all the 15 aerofoils and this data is exported and arranged in MS Excel which can be accessed using Matlab Software. [8]

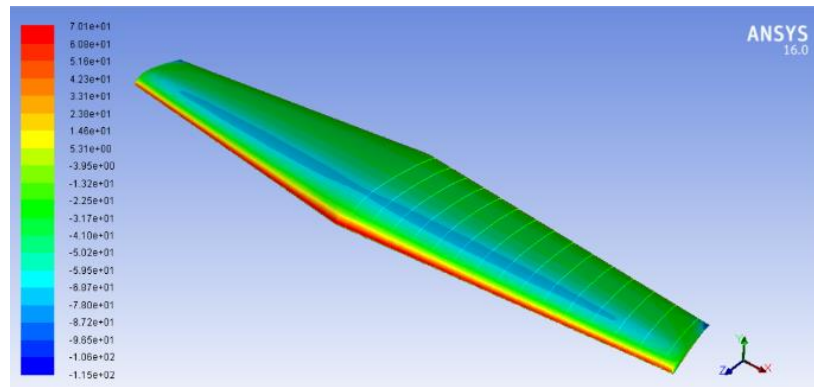


Figure 15 : Selection and Marking of aerofoils.

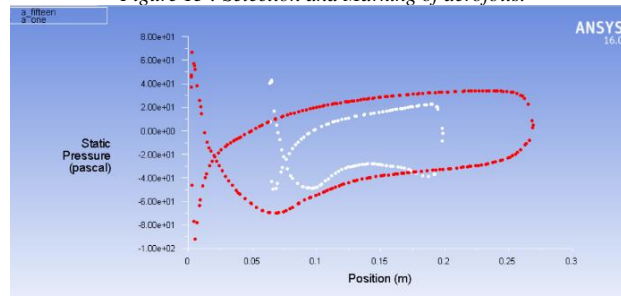


Figure 16 : Static Pressure Distribution along the chord of 1<sup>st</sup> and 15<sup>th</sup> aerofoil.

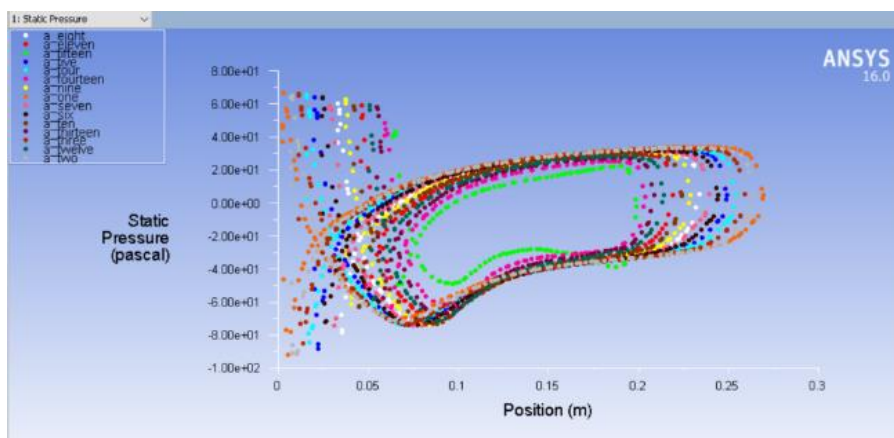


Figure 17: Static pressure distribution along the chord of all highlighted aerofoils.

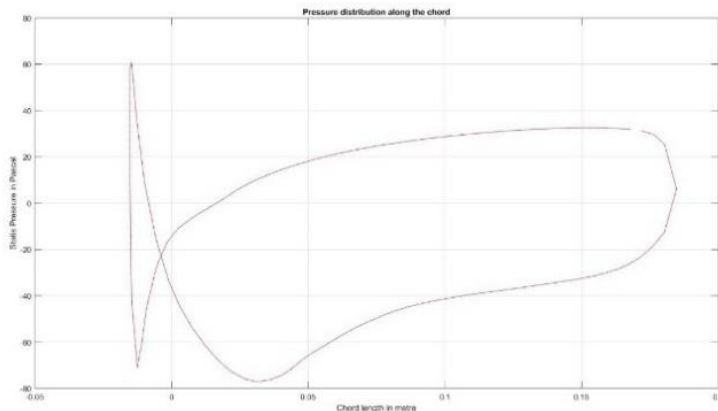


Figure 18 : Static pressure Curve exported to MS-Excel and accessed through Matlab and used for Integration.

Then, we developed a small Algorithm in Matlab software which helped us access the pressure distribution data and perform the operations in Matlab. Area enclosed in between the curve gives us the value of the integral of that function.

We plotted the graphs from the data which was exported using Ansys Fluent Software and used the self-developed algorithm to find the value of the area enclosed in between the 2 curves which denote the pressure distribution across the upper and lower parts of an air foil. We got the value of integral and then we multiplied it with the width of an air foil to find the overall lift generated by that particular block on the wing. We repeated the similar procedures and found out the lift generated by each individual block on the wing. The total lift is therefore addition of lift generated by each individual block. When we find the lift, we can easily find the Coefficient of Lift at that particular block on the wing as area of each block is already known and plot the lift distribution curve. Figure 20 and 21 depict the lift generated by each block on the half wingspan and figure 22 is the coefficient of lift distribution curve for the half wingspan.

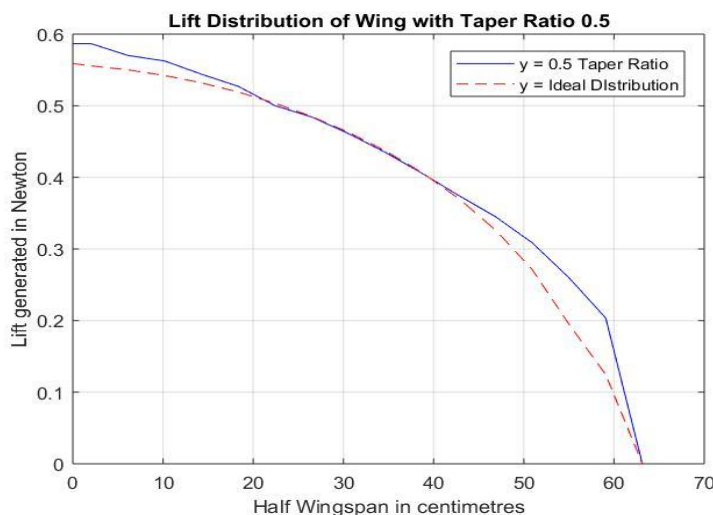


Figure 19 : Lift Distribution curve generated through Matlab.

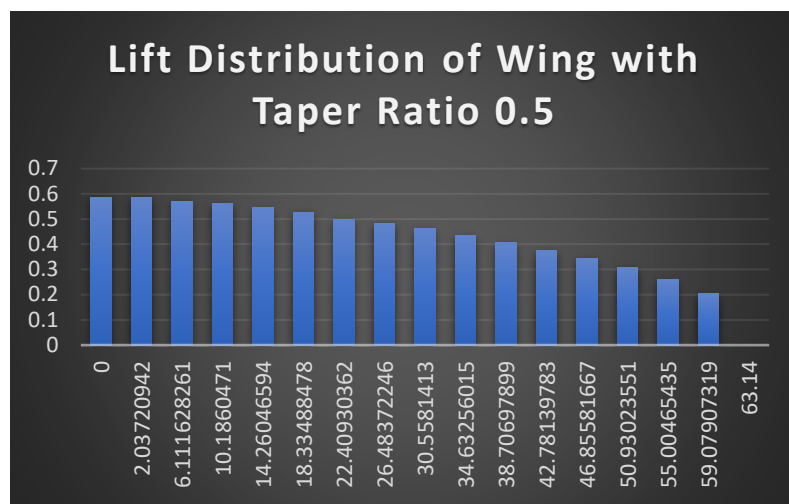


Figure 20 : Lift generated by each Individual Block

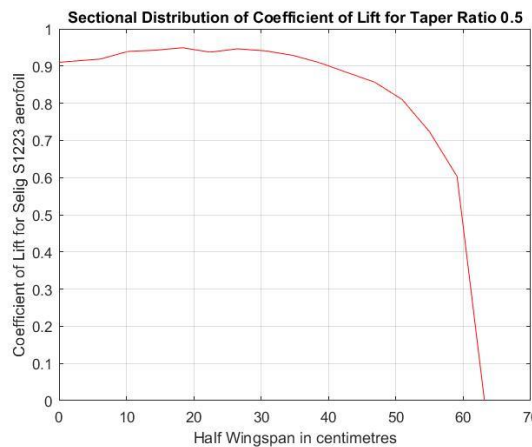


Figure 21 : Local Coefficient of Lift Distribution across the Half Wing span.

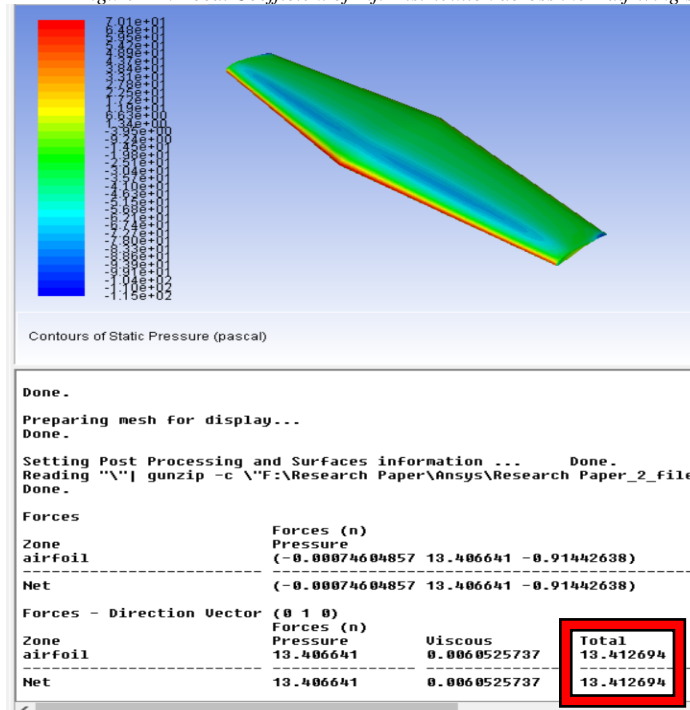


Figure 22 : Lift obtained after Analysis in Ansys CFD.

We can conclude that the results which we got through Matlab and the results from the Ansys analysis are nearly identical. The half wing according to Ansys analysis produces a lift of  $13.41N/2 = 6.705N$  and the results which we got after adding individual lift of each block was 6.568 N. Thus, we get an error of approximately 2% which is acceptable for the analysis of RC planes. If we increase the number of divisions, our accuracy will increase but the complexity increases too. Considering the optimized number of divisions, this process is acceptable and can be used to find the lift distributions of various wings. Lastly, we can find the local coefficient of lift distribution which gives us some idea about the stall patterns and other important characteristics of the plane behaviour. Accordingly, we prepared the report of all the wings and analysed it considering the various parameters and performed a detailed trade study and finalized the best combination of the wing.

### 5) RESULTS AND DISCUSSION

After the simulation of all 3D wings was complete, we analysed the results and studied them on the parameters like local coefficient of lift distribution, lift distribution, stall characteristics and structural characteristics. All the wing models have a wing area of  $2400\text{cm}^2$ , Aspect Ratio of 6, S1223 aerofoil and the simulation was carried out at a constant velocity of 10m/s. The results are as follows. Figure number 24 to 33 depicts the pressure distribution of aerofoils. Figure number 34 to 43 depicts the real lift distribution in Newton's of all the aerofoils. Figure number 44 to 53 depicts the part wise lift distribution of all the air foils. Figure number 54 to 63 depicts the real distribution of 3D Lift coefficient of all the air foils. Figure 64 to 73 depicts the part wise distribution of 3D Lift Coefficient of all the air foils. Part wise distribution graphs are just for illustration purpose as they can help us easily understand the patterns in the observations.

Sr No.	Parameter	Observation and Discussion
5.1)	<b>Lift Distribution</b>	<ul style="list-style-type: none"><li>After studying the graphs (figure 34 to figure 43), we can observe that the wing area distribution dominates the lift distribution graph. But the graph isn't particularly a straight line which suggests that other parameters do make their contribution in the process.</li><li>As the taper ratio decreases the lift generation graph turns conical and as the Taper ratio increases, it transforms into rectangular distribution, we can observe this phenomenon in the figures (34 to 43). But the transformation of conical distribution into rectangular distribution takes place with the graph taking the shape of an elliptical distribution.</li><li>The intermediate stages with taper ratio of 0.4 and 0.5 show approximately elliptical lift distribution. This particular lift distribution is the most effective lift distribution as per the proven theories because the induced drag induced in such combinations is the lowest as compared to all other lift distribution patterns</li><li>We can more easily understand the shape of lift distribution if we look at the part wise distribution figures. (figure 44 to 53).</li><li>Rectangular distribution has many cons like it generates high tip vortices and also has high induced drag which reduces the efficiency of the wing. On the other tapered wing increases the wing efficiency by reducing the tip vortices and induced drag value.</li><li>The added advantage of the Conical Lift distribution is the lower tip deflection in the wings. The conical lift distribution decreases the bending moment which is imposed on the spar and as the bending moment decreases the dimensions of spar can be reduced which in turn decreases the empty wing of the plane.</li></ul>

5.2)	Local Coefficient of Lift Distribution	<ul style="list-style-type: none"> <li>After studying the graphs (figure 54 to figure 63), we observe that as the taper ratio reduces the Maximum value of the local coefficient of lift shifts outwards away from the root towards the tip. This can also be observed from the pressure contours graph (figure 24 to figure 33). The dark blue region denotes the contours with lower pressure, as the taper ratio decreases the dark blue region tends to shift towards the tip.</li> <li>This proves that as the taper ratio is reduced the stalling tendency shifts towards the tip i.e. the Wing with Taper ratio 1 has the tendency of root stalling and the wing with Taper ratio 0.1 has the tendency of tip stalling. But tip stalling conditions can cause the tip to stall abruptly causing a loss of lift unexpectedly and can cause unexpected rolls.</li> <li>As the taper ratio differs the induced drag distribution changes accordingly; when the taper ratio is reduced the drag generated by the tip vortices is reduced and hence overall drag is reduced.</li> <li>For the taper ratios of 0.4 (figure 57) and 0.5 (figure 59) the graph of the local coefficient of lift is nearly or approximately a straight line. This means that all the wing has the same value of the local coefficient of lift. This particular condition is the exact requirement of elliptical wing distribution. All the Wing has nearly the same value of the local coefficient of lift and hence all the wing stalls at the same time. The Induced Drag generated by this wing is lowest among all the wings with similar parameters and the downwash is constant for the given span. Hence has the highest Lift/Drag ratio and the highest of the efficiency.</li> </ul>
5.3)	Structural Strength and Lift Distribution across the wingspan	<ul style="list-style-type: none"> <li>After studying the lift distribution, we can calculate the dimensions of spar required for that particular wing. For structural design of the wing we assume it as a cantilever beam and apply the loads accordingly and plot the shear force and bending moment diagram. These diagrams help us get a clear picture of the scenario and helps us to optimize the spar design.</li> <li>In a Remote-Controlled Plane spar weight is the prime consideration as majority of the empty weight comprises of the spar weight. After studying the distribution pattern, we can formulate it into a point load. The location of this point from the root chord is the deciding parameter which gives us the dimensions of the spar which are the main supporting structure of any wing as they transfer the load to the main body.</li> <li>As the taper ratio increases the lift distribution curve slightly turns into a rectangular distribution which shifts the force point towards the tip chord which in turn increases the bending moment. Greater the bending moment, bigger is the size of spar that should be used to sustain the greater bending moments. So, as the taper ratio increases the size of spars tend to increase thus increasing the empty weight.</li> <li>But as the taper ratio decreases, the chord of an aerofoil also decreases which in turn reduces the maximum thickness of an aerofoil, so the spar selection is a tedious process as a single spar cannot be inserted.</li> <li>Thus, spar selection becomes complicated as the taper ratio reduces.</li> </ul>

Pressure Contours: Figures (fig 24 to fig 33) are the pressure contours of aerofoils. They depict the pressure distribution across the wings.

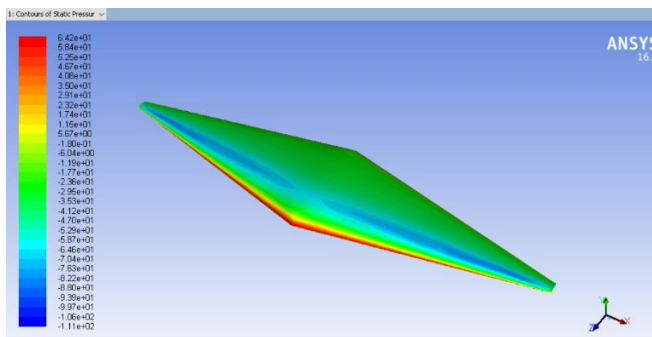


Figure 23: Taper Ratio 0.1

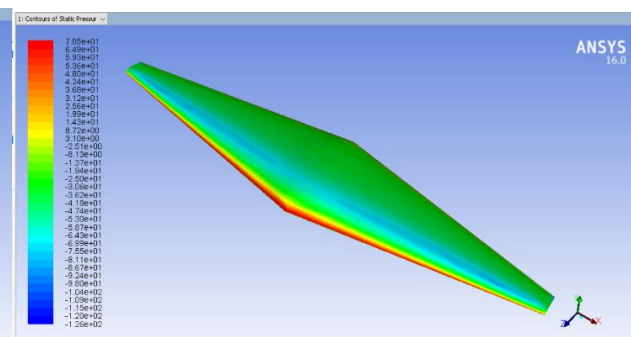


Figure 24: Taper Ratio 0.2

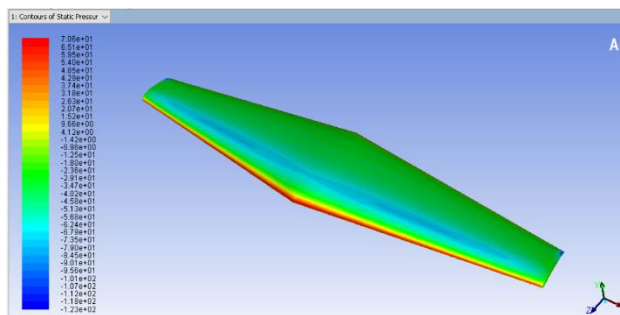


Figure 25: Taper Ratio 0.4

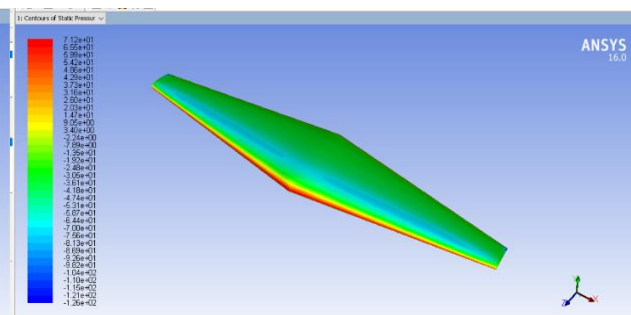


Figure 26: Taper Ratio 0.3

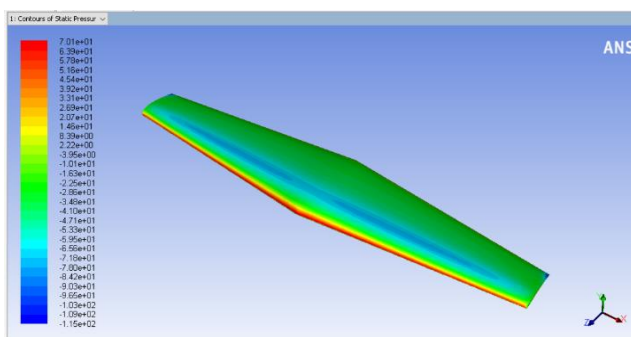


Figure 27:Taper Ratio 0.5

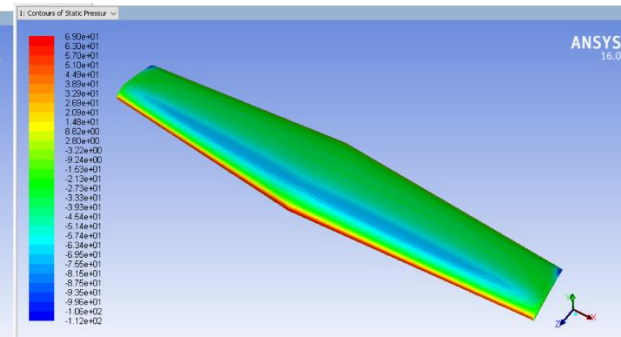


Figure 28:Taper Ratio 0.6

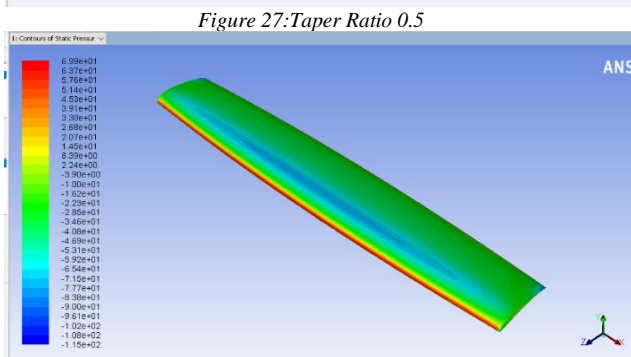


Figure 29:Taper Ratio 0.8

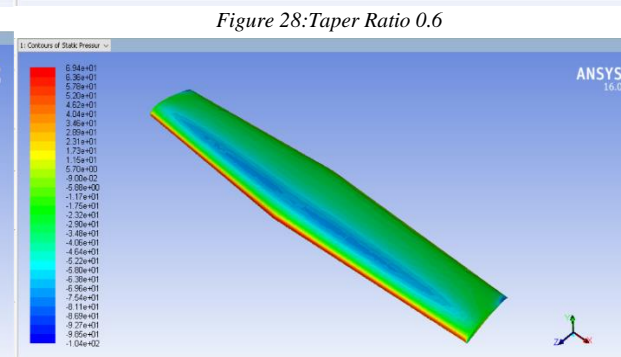


Figure 30:Taper Ratio 0.7

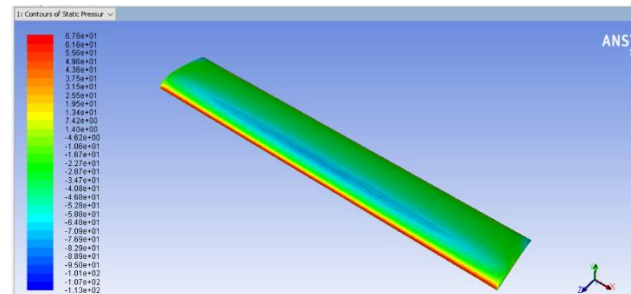


Figure 31:Taper Ratio 0.9

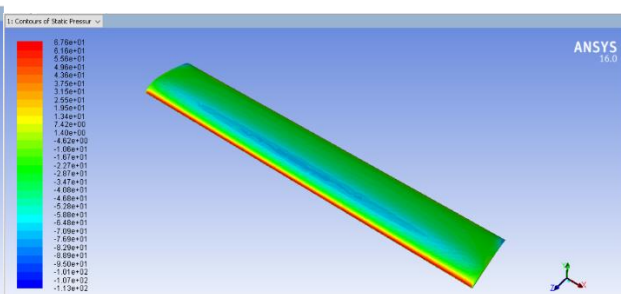


Figure 32:Taper Ratio 1

Original lift distribution: Figure 34 to figure 43 show us the real lift distribution across the half span.

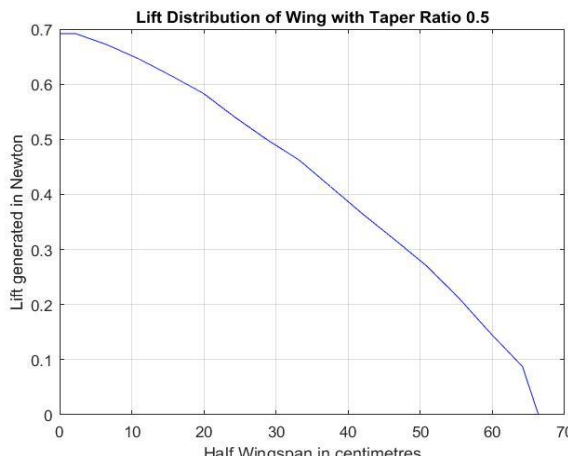


Figure 33:Taper Ratio 0.1

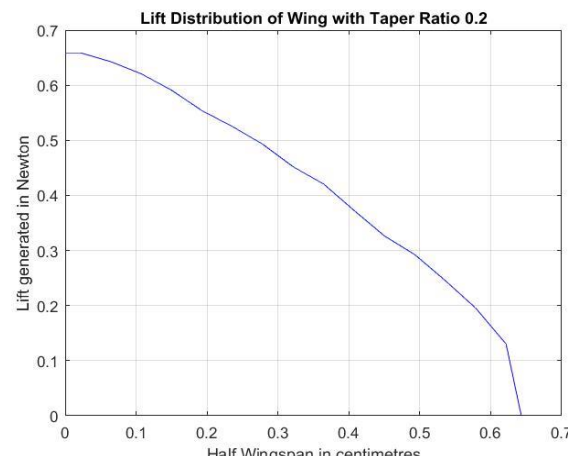


Figure 34: Taper Ratio 0.2



Figure 35: Taper Ratio 0.4

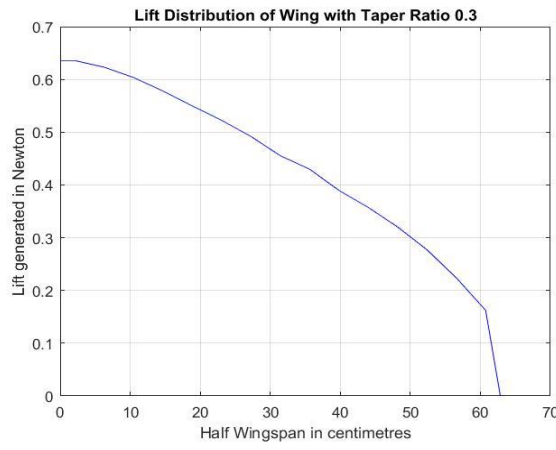


Figure 36: Taper Ratio 0.3

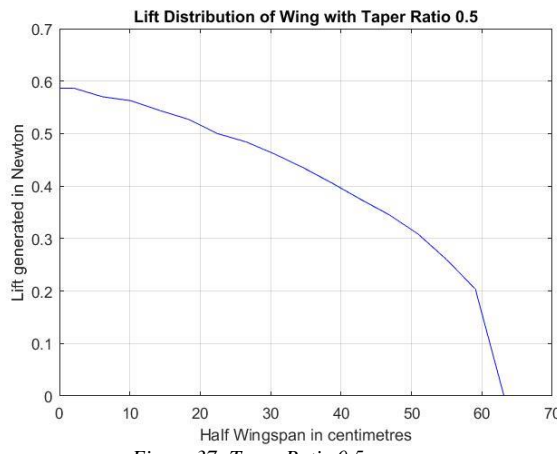


Figure 37: Taper Ratio 0.5

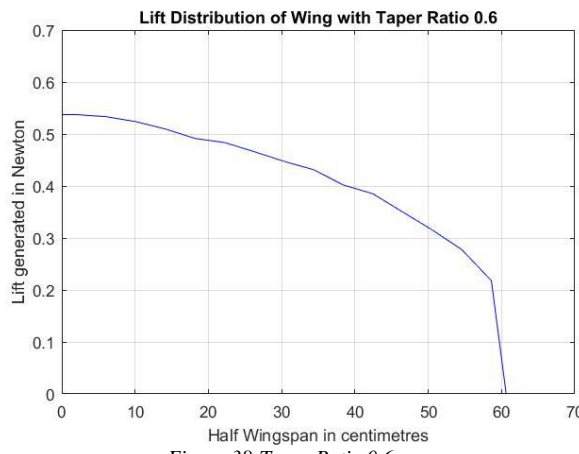


Figure 38: Taper Ratio 0.6

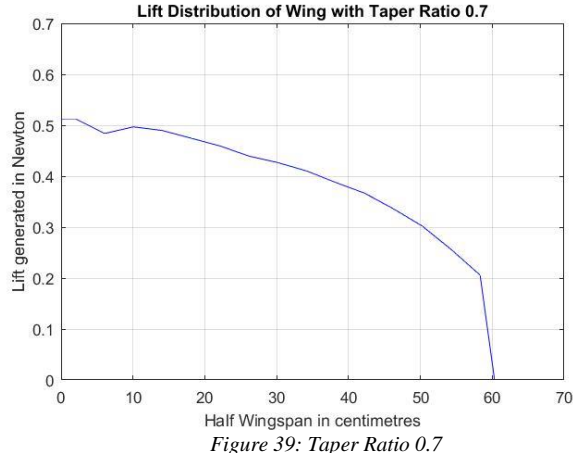


Figure 39: Taper Ratio 0.7

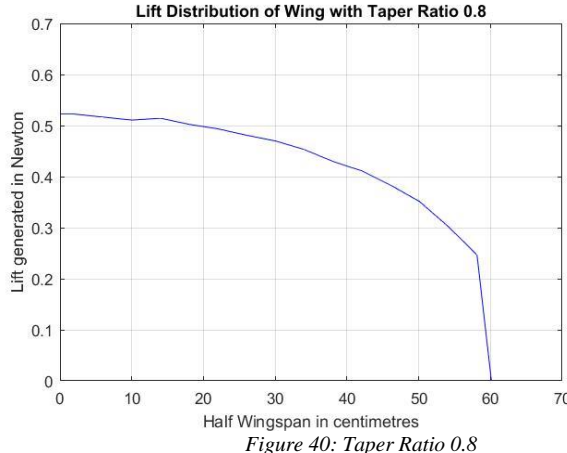


Figure 40: Taper Ratio 0.8

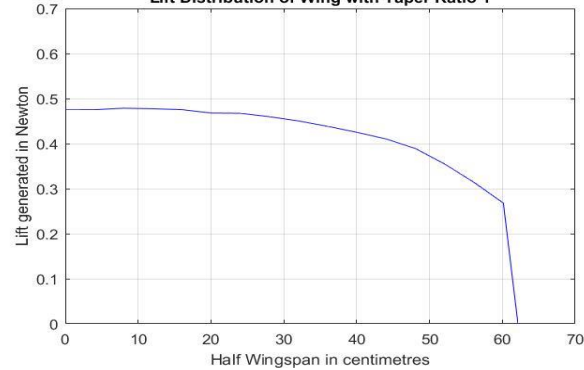


Figure 41: Taper Ratio 1

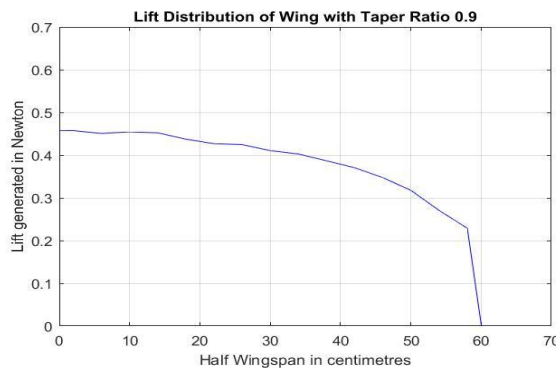


Figure 42: Taper Ratio 0.9

Part wise lift distribution: Figure 44 to figure 53 show us the part wise lift distribution across the half wing span.

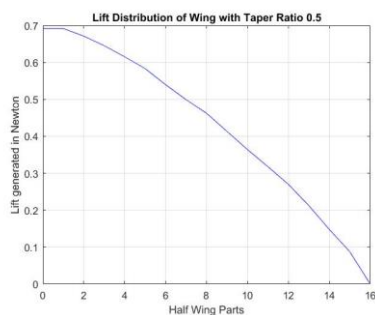


Figure 43:Taper Ratio 0.1

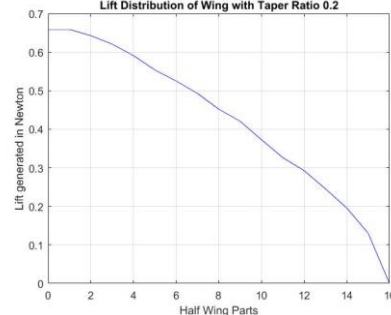


Figure 44:Taper Ratio 0.2

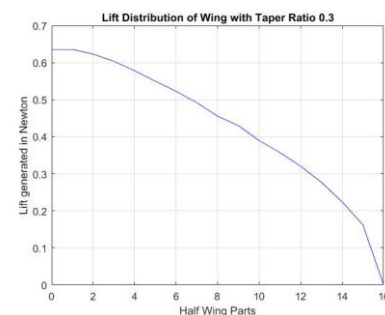


Figure 45:Taper Ratio 0.3

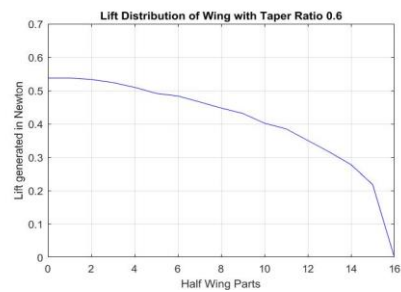


Figure 46:Taper Ratio 0.6

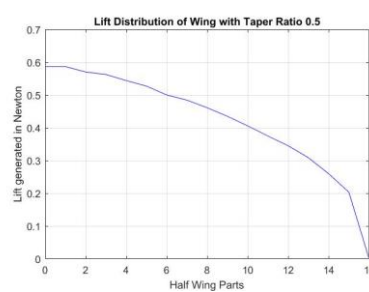


Figure 47:Taper Ratio 0.5

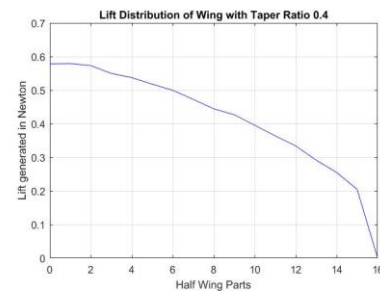


Figure 48:Taper Ratio 0.4

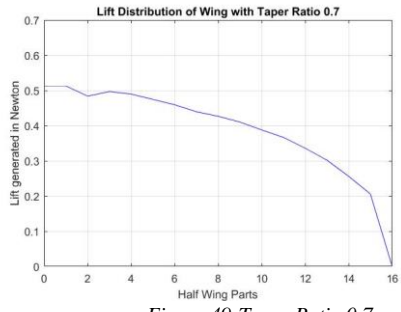


Figure 49:Taper Ratio 0.7

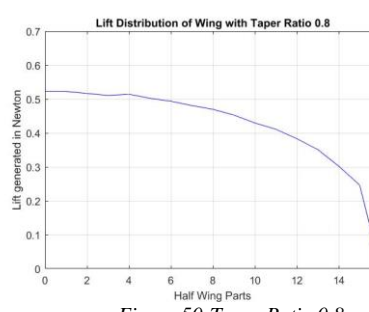


Figure 50:Taper Ratio 0.8

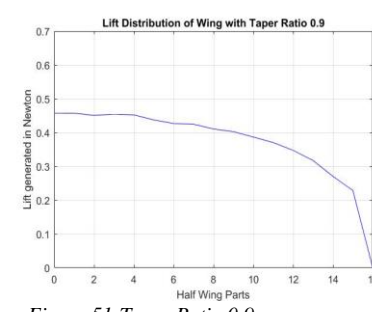


Figure 51:Taper Ratio 0.9

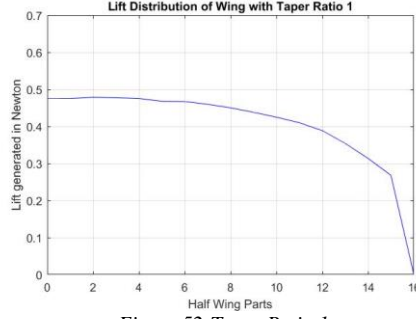


Figure 52:Taper Ratio 1

Original local coefficient of lift distribution: Figure 54 to figure 63 shows the real local coefficient of lift distribution across the half wing span.

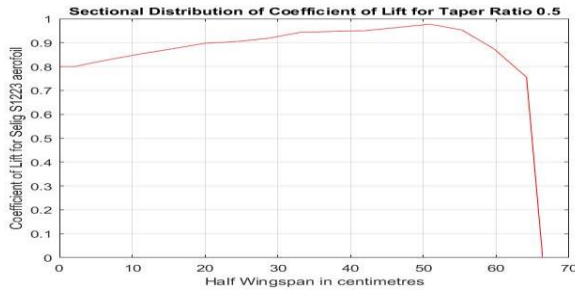


Figure 53: Taper Ratio 0.1

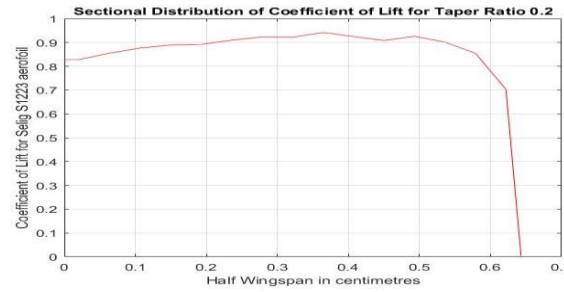


Figure 54: Taper Ratio 0.2

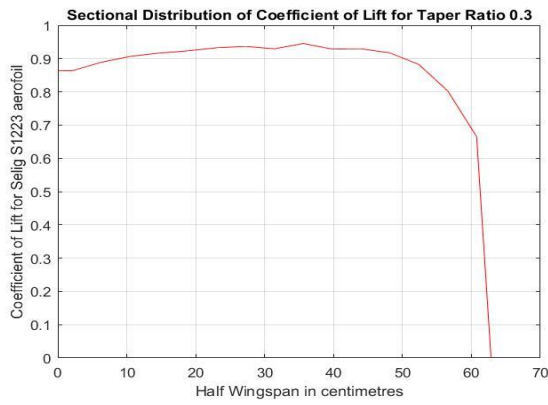


Figure 55: Taper Ratio 0.3

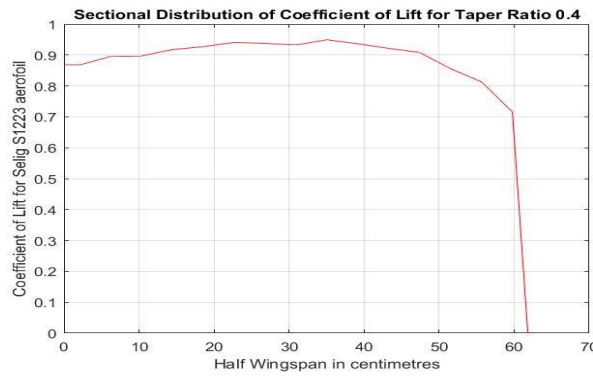


Figure 56: Taper Ratio 0.4

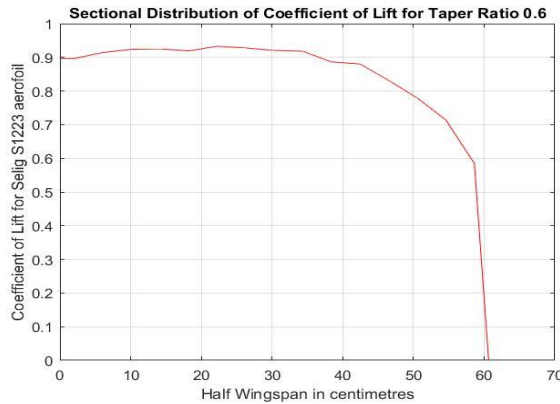


Figure 57: Taper Ratio 0.6

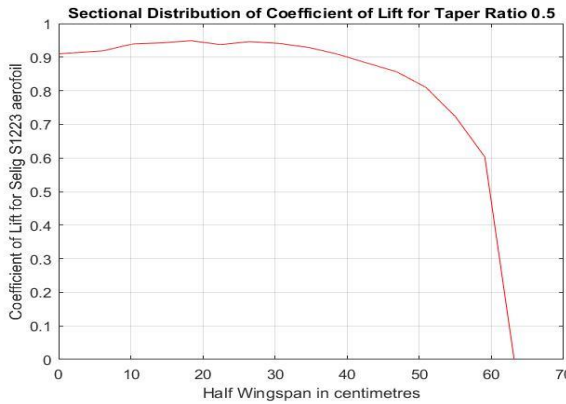


Figure 58: Taper Ratio 0.5

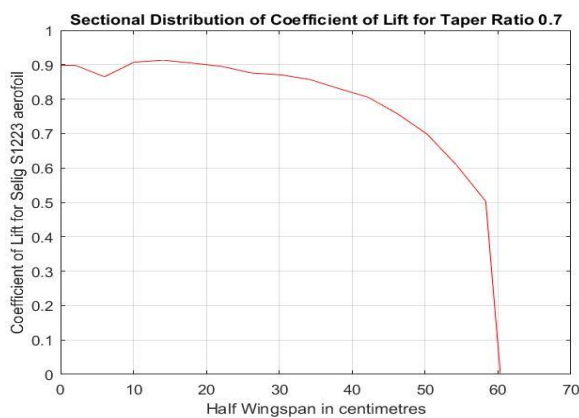


Figure 59 : Taper Ratio 0.7

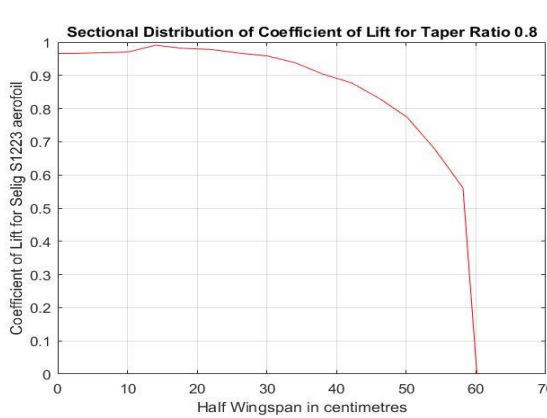


Figure 60: Taper Ratio 0.8

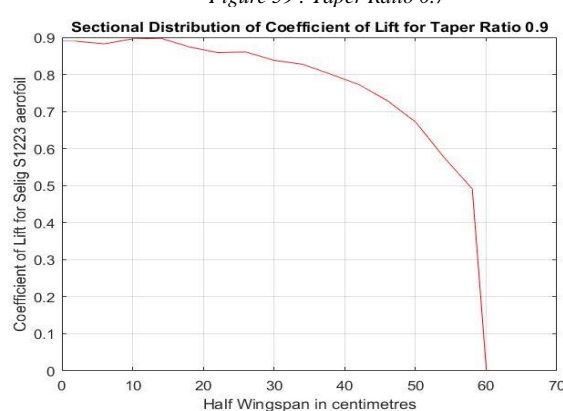


Figure 61 : Taper Ratio 0.9

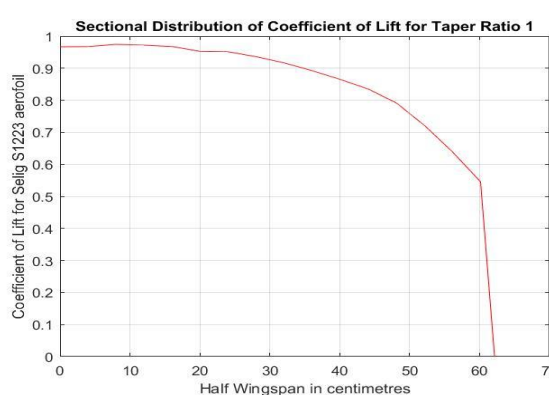


Figure 62: Taper Ratio 1

Part wise local coefficient of lift distribution: Figure 64 to figure 73 show us the part wise local coefficient of lift distribution across half wing span.

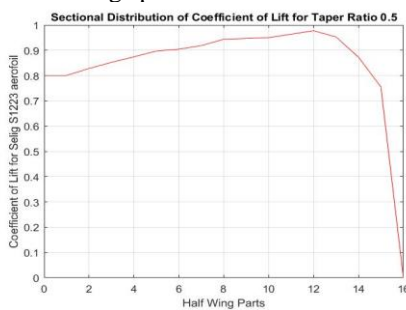


Figure 63:Taper Ratio 0.1

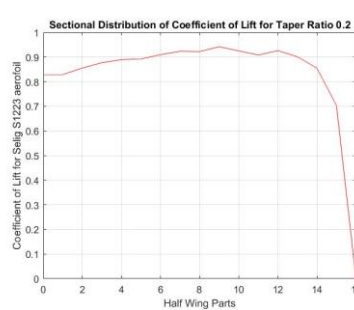


Figure 64:Taper Ratio 0.2

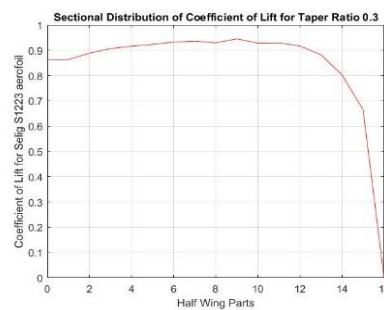


Figure 65:Taper Ratio 0.3

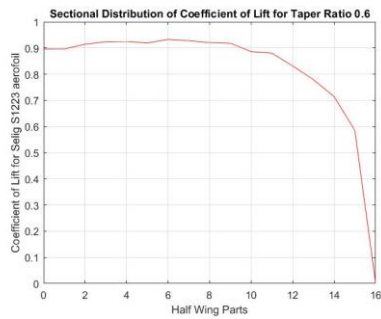


Figure 66:Taper Ratio 0.6

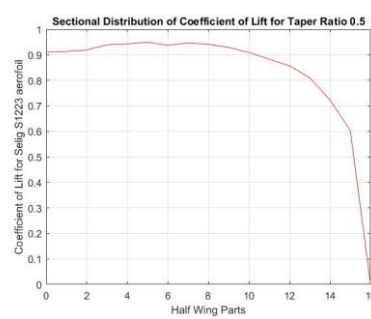


Figure 67:Taper Ratio 0.5

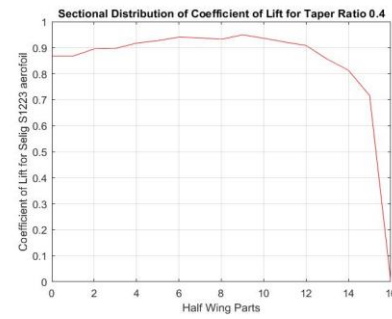


Figure 68:Taper Ratio 0.4

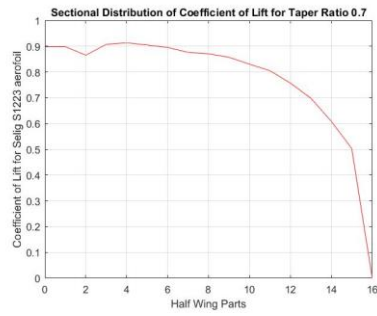


Figure 69:Taper Ratio 0.7

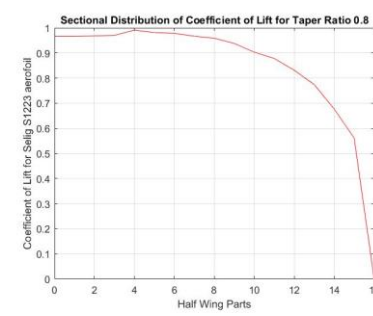


Figure 70:Taper Ratio 0.8

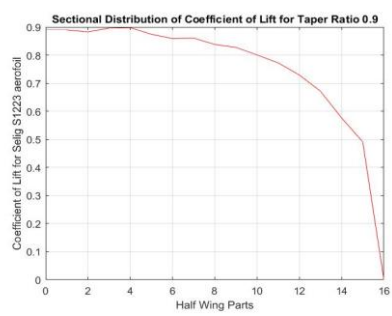


Figure 71:Taper Ratio 0.9

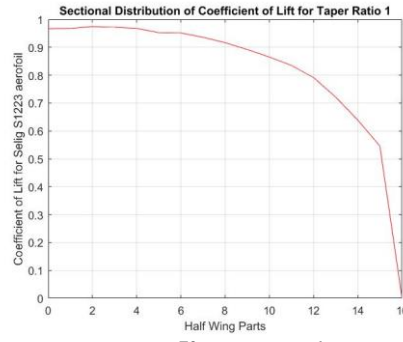


Figure 72:Taper Ratio 1

## 6) CONCLUSION

After the research, we concluded that for any RC plane a Taper Ratio of 0.4 or 0.5 might be the best possible taper ratio to go with if there isn't any sweep angle or dihedral or polyhedral angle involved. The main disadvantage of using a strong tapered wing is the very high value of local coefficient of lift at the tips which can prove fatal during the stall conditions. On the other hand rectangular wings are more stable in the stalling conditions but are not very efficient as compared to the tapered wings or elliptical wings. Wings with taper ratio 0.4 and 0.5 have near about elliptical lift distribution and according to the existing theories they are very much efficient.

This methodology which we used for plotting the graphs is tried and tested and works properly with an error of approximately 2%. This error can be minimized if the analysis is carried out with a greater number of parts. As the parts increases, the complexity of the problem increases so considering our priority 15 parts were perfect for our application. This methodology can be used for a wide number of wing designs and the results are genuine and trustworthy. We can easily get the distribution of 3D Coefficient of Lift around the span which is of great importance to any designer. The custom wing designs are possible with this approach and we can easily predict the behaviour of the wing as well as choose the properties which we desire using this approach. The Lift Distribution is useful for the Reinforcement designing and for weight reduction and weight optimization.

## 7) FUTURE SCOPE

We have assumed the wing without any twist angle or washout angle. Lower Taper Ratios can be more efficient if a certain degree of twist is provided to them. Also, the dihedral angle has certain effects on the performance of the wing. The perfect combination considering the Twist angle, Taper Ratio, Aspect ratio, Washout Angle, Dihedral angle etc can be found out using a similar methodology. This will lead us in finding the perfect efficient wing design which is more efficient and better.

## REFERENCES

- [1]] S. E. David F. Anderson, *Understanding Flight*, New Delhi: McGraw-Hill, 2001, pp. 15-95.
- [2] O. Cleynen, Artist, *Wing profile nomenclature.svg*. [Art]. 19 April 2011.
- [3] "Aviation Stack Exchange," [Online]. Available: <https://i.stack.imgur.com/WEBH6.jpg> .
- [4] [Online]. Available: [https://vignette.wikia.nocookie.net/gtae6343/images/c/c4/Induced\\_effective\\_AOAs.png/revision/latest?cb=2009101708594](https://vignette.wikia.nocookie.net/gtae6343/images/c/c4/Induced_effective_AOAs.png/revision/latest?cb=2009101708594) .
- [5] "Airfoil Tools," [Online]. Available: <http://airfoiltools.com/airfoil/details?airfoil=s1223-il>.
- [6] A. Prabhakar and A. Ohri, "Application of CFD Simulation in the Design of a Parabolic Winglet on NACA 2412," in *Proceedings of the World Congress on Engineering, WCE 2014*, London, 2014.
- [7] S. S. Sathaye, "Lift Distributions on Low Aspect Ratio Wings at Low Reynolds Numbers," WORCESTER POLYTECHNIC INSTITUTE, Worcester, 2004.
- [8] R. I. Rubel, K. Uddin, Z. Islam and M. Rokunuzzaman, "Numerical and Experimental Investigation of Aerodynamics Characteristics of NACA 0015 Aerofoil," *INTERNATIONAL JOURNAL of ENGINEERING TECHNOLOGIES Robiul Islam Rubel et al*, vol. 2, 2016.

## AUTHORS PROFILE



Mr. Tejas Dhekane : Undergraduate student at Department of Mechanic Engineering, Smt Kashibai Navale College of Engineering, Pune, Maharashtra, India.



Dr. Nitin Sherje : Head of Department of Mechanical Engineering, Smt Kashibai Navale College of Engineering, Pune, Maharashtra, India